Electroleaching of NdFeB Matrix from Spent Permanent Magnets in Organic Acids

by

Junhong Li

Student Number: 5706238
Faculty: Mechanical Engineering
Supervisor: Dr. S. T. Abrahami TU Delft

TU Delft

Electroleaching of NdFeB Matrix from Spent Permanent Magnets in Organic Acids

Junhong Li

Department of Material Science and Engineering, Faculty of Mechanical, Maritime and Materials Engineering, Delft University of Technology, Mekelweg 2, 2628 CN, Delft, Netherlands

Abstract

Neodymium (Nd) recycling plays a significant role in rare earth elements (REEs) reproduction and spent neodymium-iron-boron (NdFeB) permanent magnets is a crucial resource for Nd. This study aims at investigating the anodic behaviour and dissolution properties of NdFeB magnets during electroleaching in four biodegradable organic acids to indicate a suitable environmentally friendly and safe reagent that promotes electroleaching. Scanning electron microscopy-energy dispersive X-ray spectroscopy (SEM-EDS) characterization revealed that the metallic coating of the magnet was made of zinc. SEM-EDS analysis of polished sample surface showed the Nd-rich phases were surrounded by the matrix. Then open circuit potential (OCP) and linear scanning voltammetry (LSV) measurements were carried out to study the anodic behaviour of NdFeB. The comparison among the four organic acids at 1 M resulted in that citric acid and tartaric acid achieved the highest corrosion current with least negative OCP, as they have more carboxylic groups and higher acidities, while the lower OCP of formic acid compared to acetic acid which shows the lowest acidity revealed that the chemical leaching properties are not only dominated by acidity. But the higher corrosion current density of formic acid stated that the external potential reduced the influence of the factors other than acidity. Next, citric acid and formic acid were selected for studying the impact of concentration on anodic behaviours for their high corrosion current density and low price. Along the test that monitored the concentrations, 0.25 M citric acid was selected as the desired electrolyte for the higher corrosion current density compared to all groups of formic acid and low difference between citric acid at higher concentrations. The chronopotentiometry experiment for observing the influence of applied current density on the dissolved mass of NdFeB was failed to carry out due to the limited voltage range of the potentiostat. SEM-EDS characterization displayed that the NdFeB matrix formed a rough and porous surface after electroleaching, and the increase in test time and acid concentration promotes dissolution. The semi-quantitative composition analysis showed good dissolution properties of Nd-rich phases and praseodymium (Pr) when undergoing electroleaching in citric acid.

1. Introduction

Along the development of the modern industry, the 15 elements in the lanthanides group as well as scandium, and yttrium, the so-called Rare-Earth Elements (REEs), play an irreplaceable role in low-carbon technologies. (Liu, et al., 2023) According to statistics, the total production of REEs increased to 300,000 metric tons in 2022. (Liu, et al., 2023) The annual growth rate of global market size will reach 10.8% in 2023, based on the value of 6.58 billion US dollars in 2022. (The Business Research Company, 2023) In order to meet the demand of environmental friendly technologies and powers, REEs are utilized to produce the clean power equipment, such as wind turbines, electric motors. (IEA, 2021) These materials are also used in digital industries such as producing hard disks. (Erust, 2019) Among all 17 REEs, the demand of neodymium (Nd) in energy sector meets a solid growth, especially as neodymium-iron-boron (NdFeB) permanent magnets which are widely applied in synchronous motors in electrical vehicles, electrical bicycles, scooters etc., as they provide high power density. (IEA, 2021)

However, the global REE's production is still facing the challenge of pollutions and soil erosion in mining, and a fluctuating price due to supply chain bottlenecks as well. (IEA, 2021) Therefore, the development of recycling pathways will be necessary in order to maintain a stable supply of REE resource including Nd and reduce the environmental burden.

In the current state, the two most common methods to recycle REEs are pyrometallurgical and hydrometallurgical techniques. (Omodara, 2019) In pyrometallurgical techniques, the waste material containing REEs is pretreated by oxidative roasting in 500-950℃ to enhance the selectivity against Fe in acid leaching, (Önal M. A., 2017) in order to convert the alloying metals into Fe_2O_3 and Nd_2O_3. (Venkatesan P. V., 2018) Then acids with near stoichiometry equivalent (nHCl:nREE=3.5:1) are applied to leach the Nd^{3+} selectively, and Fe^{3+} will hydrolyse when pH is higher than 2 and precipitate as $Fe(OH)_3$. (Vander Hoogerstraete, 2014) The leached rich in Nd^{3+} is then precipitated with oxalic acid. (van der Hoogerstraete, 2014) (Venkatesan P. S., 2018) (Venkatesan P. V., 2018) Therefore, though the acid used for selective leaching can be recovered in the precipitation process, roasting process of pyrometallurgy is energy intensive. (Venkatesan P. V., 2018) In hydrometallurgy techniques, the NdFeB magnets are unselectively dissolved in abundant acid, following by selectively precipitating as fluorides, oxalates or double sulphates. (Bandara, 2016) (Venkatesan P. V., 2018) Many leaching pathways in hydrometallurgy require strong inorganic acid, such as sulphuric acid (H_2SO_4), (Yoon, et al., 2014) (Önal M. A., 2015), nitric acid (HNO_3) or hydrochloric acid (HCl). (Lee, 2013) The processes have high acid consumption, (Lyman & G.R., 1993) and require excess treatment to reduce the byproduct waste gases such as SO_2 and NO_2 that are pollutant and corrosive. (Önal M. A., 2017) The excess mineral acid can cause secondary pollution if they are not properly treated. (Mao, et al., 2022)

In order to acquire the minimum energy and chemical reagent consumption, electroleaching draws attention as an alternative to hydrometallurgy. (Venkatesan P. S., 2018) (Makarova, 2020) (Kumari, 2021) Electroleaching techniques brings better selectivity for leachates and the recovering processes. The externally applied voltage can accelerate the extraction and increase the extraction rate. (Hesami, Ahmadi, Hosseini, & Manafi, 2022) Studies have showed that electroleaching is able to extract up to 98% of the REEs in the magnet, and the product purity can be higher than 99%. (Venkatesan P. V., 2018) Several inorganic acids such as HCl (Venkatesan P. S., 2018), and H_2SO_4 (Makarova, 2020) were investigated in previous researches. On the other hand, some recent studies focused on organic acids as well. Belfqueh et al. (2023) evaluated the leaching yields for NdFeB magnet powders among four organic acids, including two monocarboxylic acids: formic acid (HCOOH) and acetic acid (CH_3COOH), a dicarboxylic acid: citric acid ($C_6H_8O_7$) and a tricarboxylic acid: tartaric acid ($C_4H_6O_6$), which can be extracted from biological sources and bear excellent biodegradability, coordinating properties and electrochemical stability. (Agence Nationale de la Recherche, 2018) (Belfqueh, 2023). Belfqueh et al.'s experiments stated that, the acetic acid had the highest leaching efficiency among the four organic acids. More than 90% REEs can be leached in 60℃, with a solid/liquid ratio within 0.5-5% by 1.6-10 mol/L acetic acid in 24 h, but this process was not selective, non-REE elements like Fe, B, Co were partially dissolved. (Belfqueh, 2023) Belfqueh et al. also stated that not only the protonation, but also chelation and ligand exchange reactions affect the leaching. Thus, besides the acidity of the acids, the stability of the metal complexes and the nature counter ions have influence as well, these mechanisms make acetic acid bear the highest

leaching yield with the lowest acidity among the four organic acids. (Belfqueh, 2023) Besides chemical leaching, Kumari et al. (2021) investigated the electrochemical dissolution of NdFeB using citric acid. The experiment found that as the applied current densities increased from 50 to 500 A/m^2 to the NdFeB magnet immersed in 0.5 mol/L citric acid for 5 h, the dissolved weight of NdFeB increased from 1.25 g to 3.88 g. (Kumari, 2021)

Based on previous literatures, the electrochemical measurements involving different types of organics require more in-depth investigations. Hence, this study aims to evaluate the anodic behaviour and the dissolution of NdFeB matrix from spent NdFeB permanent magnets in formic acid, acetic acid, citric acid, and tartaric acid during potentiodynamic polarization. HCl and H_2SO_4 will be also involved in the tests for comparison. The leaching efficiency will be evaluated as a function of the acid type, concentration, applied potential and current density. The results will indicate the most suitable organic acid to further promote electroleaching. The composition and morphology of the samples surface before and after polarization was characterized by scanning electron microscopy-energy dispersive X-ray spectroscopy (SEM-EDS) technique.

2. Experimental

2.1. Materials

Spent NdFeB permanent magnets from E-scooter rotor were used for electroleaching. Each piece of sample is 1.9cm×1.7cm×0.2cm in size. For the purpose of protecting the neodymium and iron from corrosion, the magnets from E-Scooter motors are coated by a metallic layer of zinc. (Chen, 2022)

In order to ensure that the electrochemical measurement would not be affected by the zinc coating, the samples underwent sanding with silicon carbide sandpapers of which the grids increased from #80 to #2000. The sanded samples were then cleaned in isopropanol and were polished with polishing pastes with powder size reducing from 3μm to 1μm and cleaned in acetone.

Four organic acids and two inorganic acids were utilized for studying the electrochemical behaviour. The citric acid (crystals, extra pure), tartaric acid (crystals, extra pure) and acetic acid (99-100%) were purchased from Boom B.V. The formic acid (≥96%) and sulphuric acid (95.0-97.0%) were purchased from Sigma-Aldrich B.V. The hydrochloric acid (37%) was purchased from EMSURE®.

2.2. Experimental Procedures

2.2.1. Electrochemical measurements

Electrochemical measurements, such as open circuit potential (OCP), liner sweep voltammetry (LSV), and chronopotentiometry (CP) were performed in an three-electrode cell consisting of a Ag/AgCl (3M KCl) reference electrode, a platinum counter electrode, and the work electrode was NdFeB permanent magnet samples, with exposure surface area of 0.8 cm^2. All experiments were done in room temperature. Each measurement used 80 mL of electrolyte. All the electrochemical measurements were carried out in a Biologic VSP-300 potentiostat.

Initially, the OCP was measured in 1 M of each of the organic acids for 1 h. Afterwards, anodic polarisation curves were obtained by LSV technique for each

acid, starting from 50 mV below the OCP and ending at 200 mV over OCP with a sweep rate of 1 mV/s. LSV measurements in four organic acids as well as 1 M HCl and H_2SO_4 were also recorded after a shorter OCP for 5 minutes to compare the anodic behaviour of NdFeB in organic acids and inorganic acids.

In order to investigate the anodic current as a function of different concentrations of acids and evaluate the most suitable acid and the corresponding concentration for electroleaching, two organic acids were selected according to the anodic behaviour from the LSV tests and combined with their costs. LSV measurements after a 5-min OCP measurement were carried out for a set of four concentrations 0.25 M, 0.5 M, 0.75 M and 1 M. A pH meter purchased from Metrohm® was then used to measure the pH value of the acids involved, the obtained pH value of the acids will serve as a factor for selecting the most suitable leaching reagent, since an acid that achieves same acidity with lower concentration is preferred in industry production.

Eventually, in order to observe the influence of the applied current density and the amount of leached material, the CP measurement was carried out in the selected acid. The experiment was originally designed to be conducted in two concentrations: 1 M, and the concentration determined from the previous experiments. Consulted Kumari et al.(2021)'s experiment, the current density in both groups will be set as 5, 10, 15, 20 mA/cm^2, and the measurement will last for 1 h. (Kumari, 2021) However, due to the limited potential range of the Biologic® VSP-300 potentiostat (-10V to 10V), the equipment is not able to carry out tests using high current densities. Thus, a shielding process was applied to both groups, by setting a 1-min OCP and a 1-min CP in series. The OCP test provides information about the chemical corrosion potential of the NdFeB in the acid, and the current density of the CP test will decrease from high values until it is able to run for 1 minute without exceeding the limit. Then the experiment will be conducted by starting the CP test for the NdFeB samples in the acid with desired concentration and 1 M, followed by applying the corresponding highest current density for 1 hour after a 5 minutes OCP test. In the end, record the difference of both the sample masses and the pH values of the reagent before and after the CP experiment to evaluate the leaching rate of the materials.

2.2.2. Characterization

In order to analyse the composition of the NdFeB magnet samples and the effect of the electroleaching on the morphology, a scanning electron microscope (SEM) with energy dispersive X-ray spectroscopy (EDS) provided by a JEOL JSM-IT-100 instrument was utilized to characterize the cross section of the NdFeB magnet, the polished surface morphology of the corrosion sites before and after electroleaching. All measurements were done under 20.0 kV acceleration voltage and 10 mm working distance. The cross section of the NdFeB magnet was characterized in the edge and in the matrix using back scattered electrons (BSE) to distinguish different elements. EDS point analyses were utilized to determine the semi-quantitative composition of the coating, and mapping technique was then

applied for acquiring the elemental distribution over the surface. The phase could be recognized by the ratio of the detected elements on the corresponding sites. The micrographs of secondary electrons (SE) and BSE were obtained for the polarization sites of the polished sample before and after electrochemical measurements, to investigate the polarization effect on the morphology.

3. Results and Discussion

3.1. Composition and Morphology Before Electrochemical Measurements

For the purpose of determining the chemical composition of the NdFeB samples that will undergo electrochemical leaching, a mounted NdFeB magnet cross section shown in Fig. 1(a) and a polished sample surface on which the metallic coating was removed, shown in Fig. 1(b) were scanned under SEM, and EDS was applied for obtaining their elemental composition.

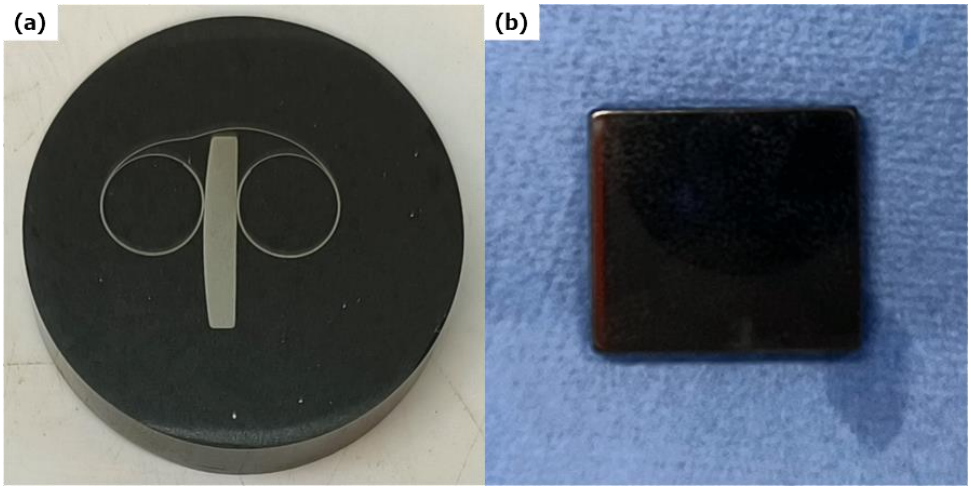

Fig. 1. (a) Mounted NdFeB magnet cross section sample; (b) Polished NdFeB magnet surface sample.

A metallic layer is coated on the NdFeB magnet to protect the Nd and Fe from corrosion. SEM-EDS were utilized to recognize the chemical composition of the protective layer by scanning on the cross section of a unpolished sample. The BSE micrograph in Fig. 2(a) showed that the thickness of the coating layer was 6.8μm in average. The analysis in Fig. 2(b) illustrated that the material used for coating was zinc.

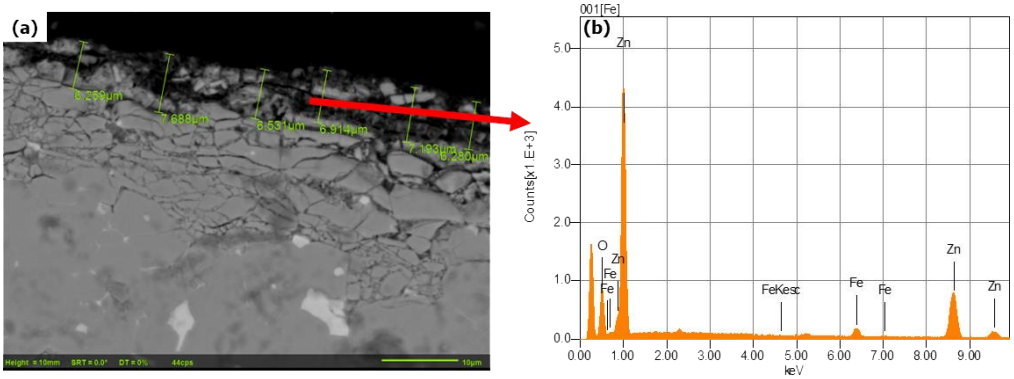

Fig. 2 (a) BSE micrograph of the NdFeB magnet cross section; (b) EDS analysis of the chemical composition of the zinc coating

After characterizing the component of the coating layer, the elemental composition within the NdFeB alloy was investigated on a polished surface using SEM-EDS mapping technique, the results were shown in Table 2 and Fig. 3. The SEM-EDS mapping of chemical contrast shows the BSE micrograph and the distribution of Fe, Nd, and O on the polished surface. The distribution of Pr was not presented in the mapping, the reason is speculated to be that the difference between the photon energies of principle K- and L-shells in Nd and Pr are lower than the energy resolution set for the SEM during mapping, and Pr is mapped as Nd in Fig. 3(c). (Lawrence Berkeley National Laboratory, 2009) Fig. 3(b) indicates that Fe distributes homogeneously on the matrix, but the concentration is low on the white phases. Nd is more concentrated on the phases corresponding to the white spots in the micrograph. The SEM-EDS point analysis carried out the result that the white phases (1) contain 47.5 wt% Nd, 34.9 wt% Fe, 14.2% Praseodymium (Pr), 2.4 wt% Copper (Cu) and 1.1 wt% Aluminium (Al). The matrix (2) consists of 74.0 wt% (72.6 at%) Fe, 21.6 wt% (8.2 at%) Nd, 4.0 wt% Carbon (C), 0.4 Al. The stoichiometry of Nd and Fe does not represent the $Nd_2Fe_{14}B$ phase. (Mishra, 1987) In the grey spots (3) on the surface, the composition of Fe and Nd is similar to the matrix but contains 2.04 wt% oxygen, indicating that the neodymium exposed in ambient environment underwent oxidation. 0.3 wt% Ca was also detected on spot (3). According to the principle emitted photon energies, the L- lines of Cu (Lα=0.93 keV, Lβ=0.95 keV) is close to the M- lines of Nd ($M_{\alpha 1}$=0.97 keV) and Pr ($M_{\alpha 1}$=0.93 keV) it is likely that part of the photons emitted from Nd or Pr were recognized as Cu by the detector. (Lawerence Berkerly National Laboratory, 2009) Al was probably detected if the detector received the energy of two photons carrying L- line energy of Fe (L_{α}=0.71 keV, L_{β}=0.72 keV) and recognized as a single photon carrying K- line energy of Al ($K_{\alpha 1}$=1.49 keV, $K_{\beta 1}$=1.56 keV) according to the mechanism of X-ray photon emission. (Hodoroaba, 2020) (Lawerence Berkerly National Laboratory, 2009). The presence of Ca (Lα=0.34 keV, Lβ=0.34 keV) is inferred to be originated from the detector that recognized a single Fe photon carrying L-line energy as two photons emitted from the L-lines of Ca. (Lawerence Berkerly National Laboratory, 2009) The carbon signals are suspected to be arrtibuted to hydrocarbon contamination. (Postek, 1996)

In NdFeB, the oxide Nd_2O_3 and Fe_2O_3 can combine and form $NdFeO_3$. (Belfqueh et al., 2023) These mixed oxides are worth considered that they may reduce the leaching rate of Nd, due to the low solubility in mild conditions. (Jiang et al., 2020) (Jakobsson et al., 2016)

Because the principle of EDS technique to distinguish different elements is by exciting the electrons in the inner shells and eject them, then detect the energy of the X-ray emitted from the electron in the outer shells when filling the vacancies in the inner shells. (Hodoroaba, 2020) EDS has low accuracy in detecting the light elements which have low number of energy levels. (von Harrach, et al., 2010) The boron content was not detected in this study. According to previous studies of which the samples contain similar iron and neodymium content, the amount of boron is 0.9-1.00 wt%. (van der Hoogerstraete, 2014) (Belfqueh, 2023)

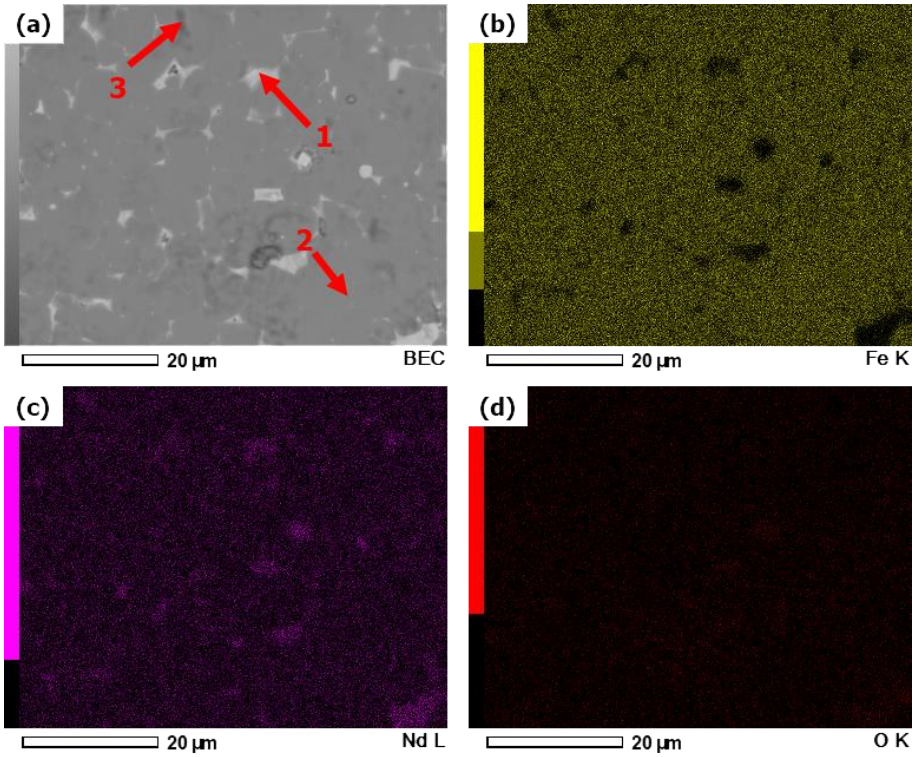

Fig.3 (a) SEM micrograph and EDS mapping of (b) iron, (c) neodymium, and (d) oxygen on the polished NdFeB magnet surface, displaying the disintegration of phases. Point 1, 2, 3 are the spots where EDS point analyses were performed.

Table 2. Semi-quantitative elemental composition (wt%) detected by EDS point analyses 1-3 in Fig. 3

Elements	1 (White)	2 (Matrix)	3 (Grey)
Nd	47.5	21.6	19.7
Fe	34.9	74.0	72.9
Pr	14.2	/	/
C	/	4.0	5.2
O	/	/	2.0
Cu	2.4	/	/
Ca	/	/	0.3
Al	1.1	0.4	/

3.2. Electrochemical measurements

3.2.1. Open Circuit Potential and Linear Scanning Voltammetry

In order to study the anodic behaviour of NdFeB when undergoing electroleaching in different organic acids to guide the selection of the suitable acids for further experiments on the influence of concentration. OCP measurement was performed for 1 h to state the free corrosion potential in four 1 M organic acids. A LSV scanning was then followed based on the potential range delimited by the OCP test. Another LSV test after a 5 min OCP test was also performed on each of the four organic acids to find out the influence of OCP testing time on the surface anodic

behaviour, two strong inorganic acids: HCl and H_2SO_4 were also tested to compare the anodic behaviour.
The obtained OCPs and the corrosion current densities (denoted as i_{corr}) recorded at -0.45 V (Ag/AgCl) are listed in Table 3.

Table 3. The open circuit potentials (as corrosion potentials) and corrosion current densities obtained at -0.45 V (Ag/AgCl) for NdFeB evaluated from the OCP and LSV measurements.

Electrolyte	*pK_{a1} (25°C)	OCP [V (Ag/AgCl)] (1h)	OCP [V (Ag/AgCl)] (5 min)	i_{corr} (A/cm^2) after 1 h OCP	i_{corr} (A/cm^2) after 5 min OCP
1 M Formic Acid	3.745	-0.59	-0.63	0.10	0.10
1 M Acetic Acid	4.6	-0.57	-0.61	0.04	0.04
1 M Citric Acid	3.1	-0.53	-0.53	0.08	0.07
1 M Tartaric Acid	2.98	-0.51	-0.52	0.11	0.10
1 M Hydrochloric Acid	-5.86	/	-0.53	/	3.90
1 M Sulphuric Acid	-2.8	/	-0.52	/	5.19

*pK_{a1} values (Smith & Martell, 1989) (Goldberg et al., 2002, pp. 231-370) (Papagianni, 2007) (Kliewer et al., 1967) (Trummal et al., 2016) (Haynes, 2014)

OCP is the voltage between the working electrode (NdFeB) and the reference electrode (Ag/AgCl) without providing external current, which reflects the equilibrium potential during reaction and thus indicating the corrosion potential that delimits the range of LSV.
When reacting with acid, Nd and Fe are oxidized by the H^+ ions and form Nd^{3+} and Fe^{2+}. The hydrogen ions are reduced into H_2 gas. Following the reaction: (Haynes, 2014)
$Nd \rightleftharpoons Nd^{3+} + 3e^- \ (eq.1), E^0_{ox} = 2.323V \ (SHE)$
$Fe \rightleftharpoons Fe^{2+} + 2e^- \ (eq.2), E^0_{ox} = 0.44V \ (SHE)$
$2H^+ \rightleftharpoons H_2(g) \ (eq.3), E^0_{red} = 0V \ (SHE)$
*The standard oxidation and reduction potentials are retrieved from (Haynes, 2014).
The recorded OCPs as a function of time are presented in Fig. 3. As listed in Table 3, tartaric acid has the least negative potential, followed by citric acid, the order matches the acidities, as the pK_a value of tartaric acid lower than the pK_a of citric acid. However, the OCP of acetic acid is 20 mV less negative than formic acid, while the acidity of acetic acid is the lowest among the acids involved. The discrete data points that are more positive before 1742s in acetic acid and citric acid are inferred to be the noise caused by random errors.

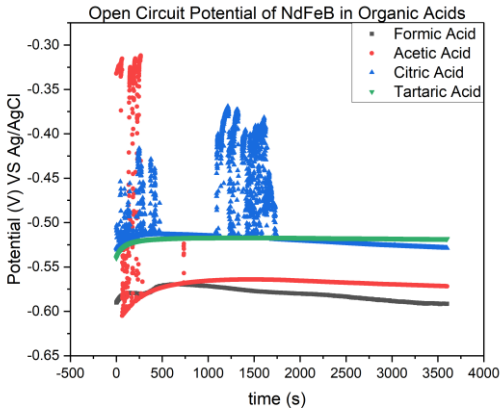

Fig. 4 The open circuit potential of NdFeB in 1 M organic acids for 1 hour.

As Belfqueh et al. (2023) concluded, the factors affecting the leaching is not only dictated by the acidities. Chelation and ligand exchange reactions also have their impact. The stability of the metal complexes and the nature counter ions have influence as well as the acidity. (Belfqueh, 2023) Therefore, the OCP of formic acid shows a decreasing trend as the reaction goes on and is more negative than the OCP of acetic acid.

The anodic current recorded in the LSV tests after 1 h OCP and 5 min OCP are shown in Fig 4. A higher current density on the anodic branch indicates a higher electron transfer rate turning more REE atoms into ions, that promotes leaching. Therefore, a higher anodic reactivity is achieved. It can be perceived from Fig. 4 that NdFeB did not passivate in all acid electrolytes during polarization. The corrosion current density recorded at -0.45 V (Ag/AgCl), where the anodic branches were fully developed, of two set of measurements are listed in Table 3. Among the four organic acids, the corrosion potential for the tests in formic acid and acetic acid after 5 min OCP tests are 0.04V lower than those after 1 h OCP tests, while for citric acid and tartaric acid, the difference in potential is lower than 0.01 V. The relationship between the data of citric acid and formic acid matches the result obtained in Kumari (2021)'s study. (Kumari, 2021)

Among the four organic acids, acetic acid bears the lowest anodic current, which is 0.04 A/cm^2, half of the current density in citric acid. However, the differences among all anodic current densities are lower than 10 mA/cm^2. As comparison, Sueptitz et al. (2010) did LSV measurement for NdFeB spent magnets in H_2SO_4, which is an inorganic strong acid. (Sueptitz et al., 2010) The anodic current densities recorded at 0.5 V were 40-100 mA/cm^2 and 0.25-0.5 mA/cm^2 corresponding to 0.005 M and 0.1 M, and the detected OCPs were (-815)-(-770) mV (SHE) and (-1088)-(-1070) mV (SHE) corresponding to 0.005 M and 0.1 M. (Sueptitz et al., 2010) For verification, in this study, 1 M HCl and H_2SO_4 were used as LSV electrolytes after 5 min OCP tests as well. The data in Table 3 indicated that the differences between the corrosion potential of HCl, H_2SO_4 and citric acid, tartaric acid are less than 10 mV, but the resulted current of the two acids 5.19

A/cm^2 for HCl and 3.90 A/cm^2 for H_2SO_4, which is 51.9 and 39 times higher than the current density of tartaric acid. The full protonation of these two strong acids provided high acidity represented as minus pK_a values in Table 3. The properties of H_2SO_4 in the experiment deviated from Supetitz et al. (2010)'s results. The reasons causing the deviation is supposed be originated from many factors, Supetitz et al. (2010) had purged nitrogen into the electrolyte for 1 h before starting the measurement, while no deaeration process was taken in this study and the residual oxygen in the electrolyte has the possibility to contribute to the oxidation. Other factors, such as stirring rate, temperature and whether the NdFeB samples underwent demagnification will also affect the electrochemical features. (Kumari, 2021)

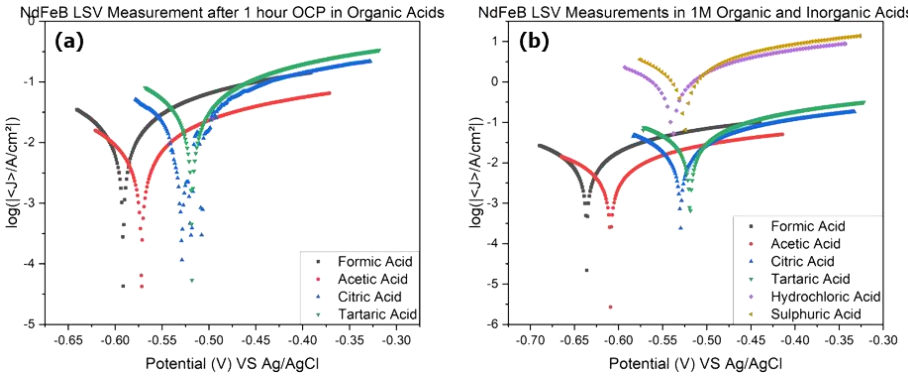

Fig. 5 Anodic polarization curves of NdFeB in 1 M acids obtained from (a) LSV after 1 h OCP measurements; (b) LSV after 5 min OCP.

For the purpose of selecting the suitable acids for further studies about the impact of concentration on anodic behaviours, the data measured in the OCP and LSV tests are taken into comparison. The anodic current densities recorded at -0.45 V (Ag/AgCl) were treated as indices to evaluate the reactivity. Hence, considered that the anodic current density of formic acid is at the same level as tartaric acid, formic acid is selected. Acetic acid, of which the corrosion current density was 0.06 A/cm^2 lower than the highest current density produced by tartaric acid according to the LSV after 5 min OCP, was eliminated. In Belfqueh et al. (2023)'s experiment, acetic acid bears the highest chemical leaching rate. (Belfqueh et al., 2023) In contrast, the external potential applied weakened the influence of counter ions and metal complexes, as the Nd and Fe on the anode are enforced to oxidize. Among citric acid and tartaric acid, these two strongest organic acids have close open circuit potential and anodic current. The differences are 0.01 V in OCP and 0.03 A/cm^2 in i_{corr} in the LSV test after 5 min OCP. According to Polsinelli® winery cooperation, the wholesale price of citric acid is £142.00/25kg, which is 69% cheaper than the price of tartaric acid: £458.00/25kg (09.25.2023). Taken the cost into consideration, eventually, formic acid and citric acid were selected for the further studies about the relationship between the electrolyte concentration and anodic behaviour.

The concentrations set for the measurements are 0.25 M, 0.5 M, 0.75 M and 1 M.

Polished NdFeB samples were used as anodes and apply LSV tests after a 5-minute OCP test. Then the OCP, recorded as the free corrosion potential and the corrosion current density recorded at -0.50 V (Ag/AgCl) for formic acid and -0.40 V (Ag/AgCl) for citric acid, where the anodic branches were fully developed, were listed in Table 4. For both acids, the differences in OCP are lower than 0.05V and the differences in i_{corr} are lower than 53 mA/cm^2. Additionally, an exceptional phenomenon occurred in both acids: the OCP and i_{corr} of NdFeB in 0.5 M formic acid are higher than the other concentrations, while in the other tests (0.25 M, 0.75 M, 1 M), the OCP and i_{corr} increased with concentration. Among the tests for citric acid, 0.75 M concentration resulted in the highest OCP and i_{corr}. However, the differences in OCP are all below 50 mV and the differences in current densities are below 50 mA/cm^2.

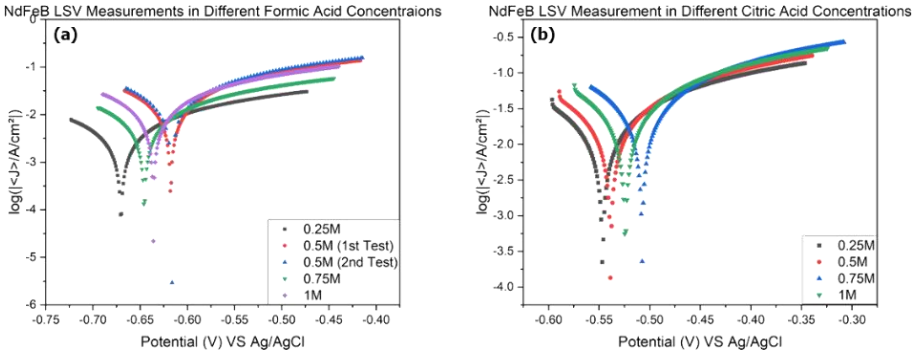

Fig. 6 The anodic polarization curves of NdFeB obtained from LSV tests after 5 min OCP in 0.25 M, 0.5 M, 0.75, 1 M (a) Formic Acid, (b) Citric Acid, under 1 mV/s scanning rate.

Table 4. The OCP and anodic current densities of NdFeB undergoing LSV tests recorded at -0.50 V (Ag/AgCl) for formic acid, -0.40 V (Ag/AgCl) for citric acid, in different concentrations of formic acid and citric acid.

Electrolyte Concentration	OCP [V (Ag/AgCl)] For Formic Acid	OCP [V (Ag/AgCl)] For Citric Acid	i_{corr} (A/cm^2) For Formic Acid	i_{corr} (A/cm^2) For Citric Acid
0.25 M	-0.67	-0.55	0.03	0.10
0.5 M	-0.62	-0.54	0.08	0.12
0.75 M	-0.65	-0.51	0.04	0.14
1 M	-0.64	-0.52	0.07	0.14

Among the electrochemical behaviour of the two acids in four concentrations, the corrosion current density produced by 0.25 M citric acid is higher than all current densities produced by formic acid, ensuring a higher electron transfer rate that is more conducive to material dissolution. As the difference in the i_{corr}s of citric acid are lower than 0.04 A/cm^2, 0.25 M citric acid was selected as the electrolyte

for studying the impact of current density on the dissolution of materials. The chemical properties are taken into evaluation additionally, as the pH value of 0.50 M, 1 M formic acid and 0.25 M, 1 M citric acid were measured and compared as Table 5. It can be concluded that the pH value of 0.25 M citric acid is lower than 0.5 M formic acid, so that less citric acid can reach higher acidity as well. This result matches the relationship of pK_a values in Table 3. (Papagianni, 2007) (Smith & Martell, 1989)

Table 5. The pH value at 23℃ of different concentration of formic acid and citric acid.

Electrolyte	Concentration	pH at 23℃
Formic Acid	0.50M	2.5
	1 M	1.8
Citric Acid	0.25 M	2.3
	1 M	1.5

3.2.2. Influence of Current Density on Leaching Behaviours

After the 0.25 M citric acid was chosen as the electrolyte for electroleaching, CP measurements were carried out in order to discover the influence of applied current on the anode on the leaching behaviour, especially the weight loss of the NdFeB magnet. The experiment was designed to set the current density as 5, 10, 15, 20 mA/cm^2 for both 0.25 M and 1 M citric acid for 1 h, consulting Kumari et al. (2021)'s study. But the potential range of the Biologic® VSP-300 potentiostat used in this study is limited within -10 V to 10 V. A shielding process was therefore taken by setting a 1-min OCP and a 1-min CP in series to locate the highest current available without exceeding the limit. The shielding process resulted that the highest current applied to NdFeB in 0.25 M citric acid is 7 mA, and 12 mA for 1 M citric acid. As the surface area of the NdFeB sample is 0.8 cm^2, hence the current density is 8.75 mA/cm^2 for 0.25 M citric acid and 15 mA/cm^2 for 1 M citric acid. In practice, however, both of the groups failed to run the experiment for 1 h. The test in 0.25 M citric acid lasted for 133 s, and the test in 1 M citric acid lasted for 268 s. The mass loss and the change in pH values in the two tests were listed in Table 6. Compared to 0.25 M citric acid and the current density of 8.75 mA/cm^2, NdFeB in 1 M citric acid and 15 mA/cm^2 current density dissolved three times of materials. However, the mass difference was on the order of 1×10^{-3} g. Such difference is lower than the errors obtained in Makarova (2020)'s study. (Makarova, 2020) Two varieties were monitored in the experiment, therefore is unable to analyse the impact of neither current density nor acid concentration on the leaching behaviour. Additionally, since the test time of the two groups were 3.6% (8.75 mA/cm^2) and 7.4% (15 mA/cm^2) of the originally set time, a current density able to run for 1 h for both groups is predicted to be too low to be applied in industry production. Hence, no valid data could be observed through the equipment setup in the study, potentiostats with broader volage ranges are required to be conducted in further investigations.

Table 6. The mass loss and change in pH value for NdFeB underwent chronopotentiometry measurement in 0.25 M, 1 M citric acid at 23℃

Citric Acid Concentration (M)	Current Density (mA/cm^2)	Mass Loss (g)	Initial pH	Final pH	pH Change
0.25	8.75	0.0008	1.85	2.33	0.48
1	15	0.0024	1.49	1.80	0.31

3.3. Composition and Morphology After Electrochemical Measurements

The morphology of the NdFeB magnet before and after polarization is presented in Fig. 7. After electroleaching, the anode region reacted with acid became rough and porous (Fig. 7b). The surface of the magnet was broken down, and the average diameter of the granules are 4.6 μm. The impact of the leaching time on the morphology is indicated as Fig. 8, where the surface of NdFeB magnets underwent LSV after 5 min OCP test and 1 h OCP test were scanned. More surface breakdown and a higher porosity is observed as the exposure of internal granules increases when the leaching time extends from 5 min to 1 h. The influence of acid concentration is discovered in Fig. 9 as well, by comparing the surface micrograph of a NdFeB magnet sample underwent LSV measurements after 5 min OCP tests in 0.75 M and 1 M citric acid. A higher breakdown degree on the surface is obtained in the sample leached in 1 M citric acid. It can be concluded that longer leaching time and higher acid concentration will promote the dissolution of NdFeB.

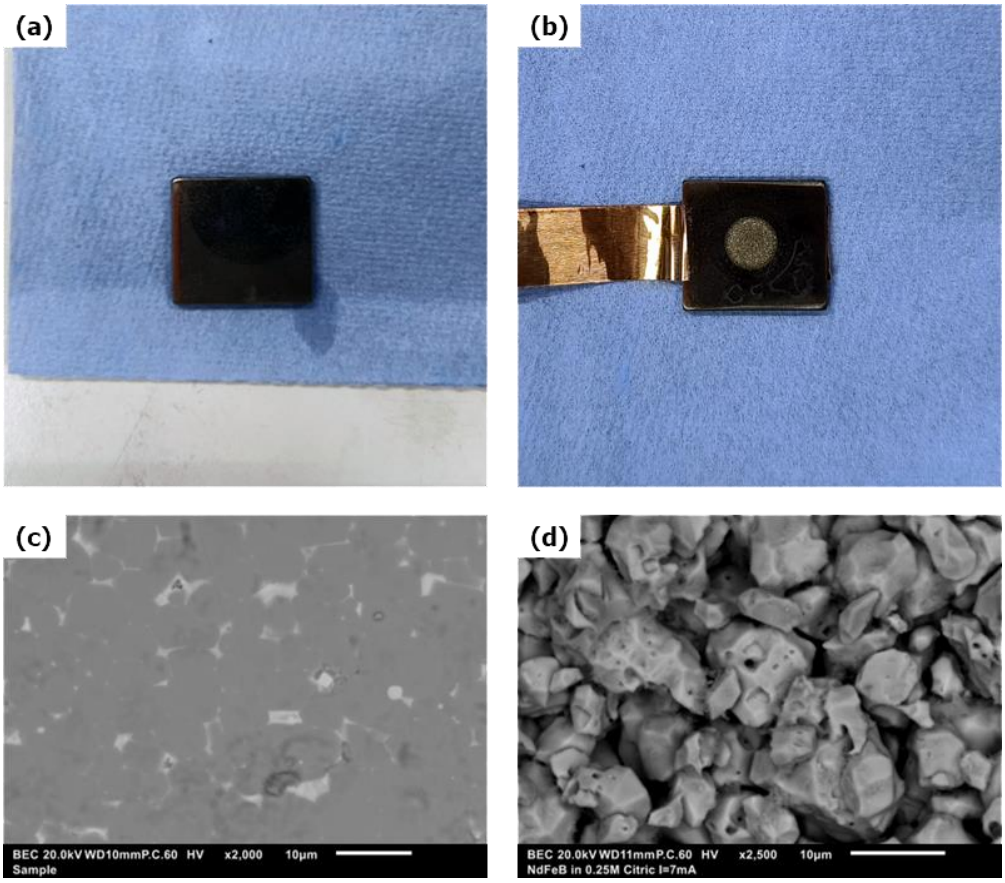

Fig. 7 (a) Polished NdFeB magnet sample before electroleaching, (b) A sample after LSV measurement in 0.5 M formic acid after 5 min OCP test, (c) BSE micrograph of a polished NdFeB magnet surface, (d) BSE micrograph of the polarized sites.

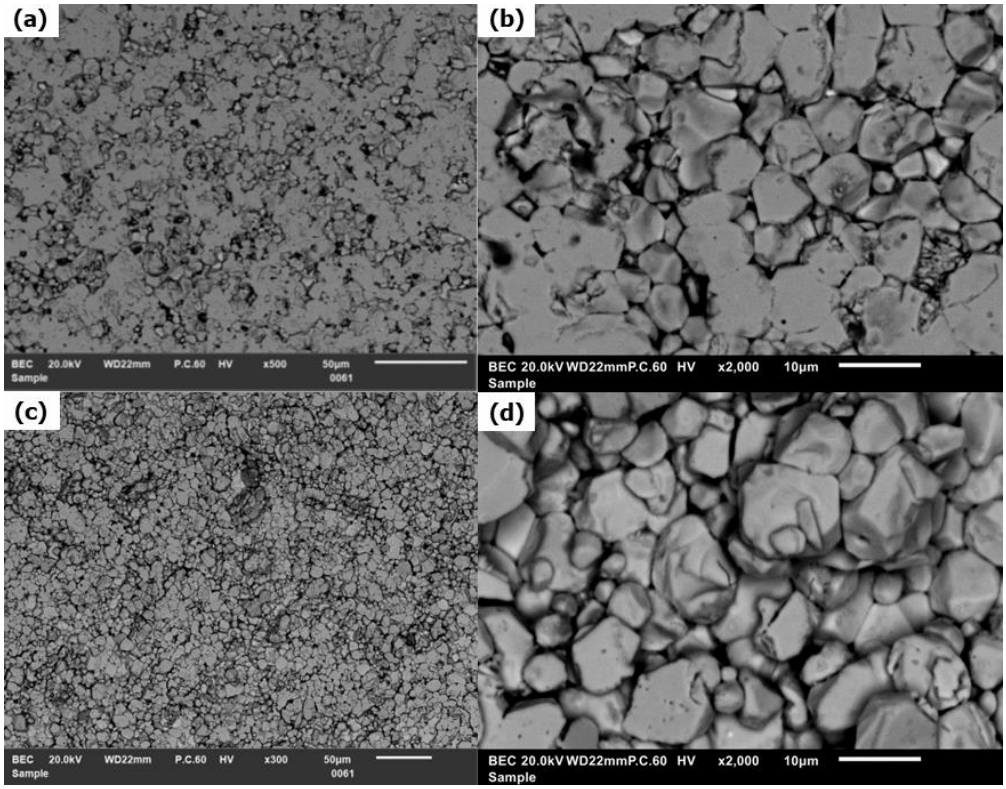

Fig. 8 BSE micrographs of NdFeB sample underwent LSV test in 1 M citric acid after (a)(b) 5 min OCP measurement; (c)(d) 1 h OCP measurement.

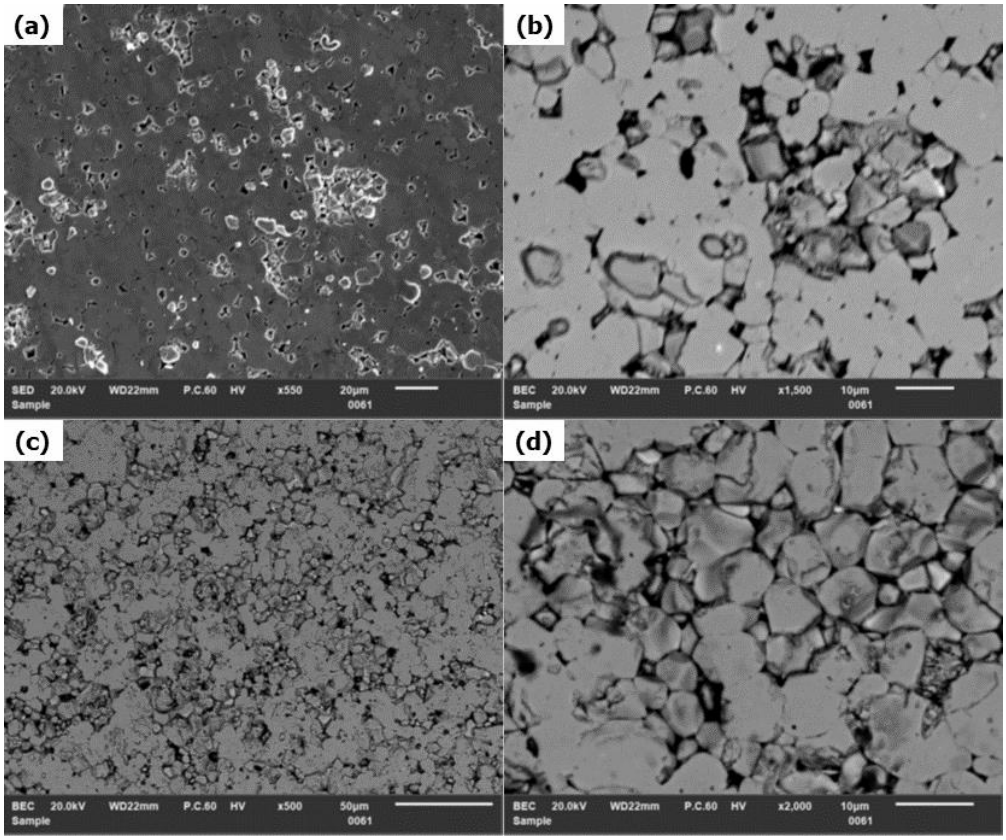

Fig.9 SEM micrographs of NdFeB sample underwent LSV test after 5 min OCP measurement in (a)(b) 0.75 M citric acid, (c)(d) 1 M citric acid.

SEM-EDS analyses were performed on three sites of the polarized site on a sample 0.25 M citric acid with 7 mA/cm^2 external current density applied for 133 s: (1) a cavity among the granules, (2) a white spot on the granule, and (3) a white matrix, as indicated in Fig. 10. The result in Fig. 8 and Table 7 showed that no Pr were detected on the surface of polarization sites, and Nd-rich sites which appeared in Fig. 2 did not exist after corrosion as well.

Another NdFeB sample underwent LSV measurement after 5 min OCP test in 1 M citric acid was analysed as well. As indicated in Fig. 11, the composition of four sites on the surface were (1) a white spot on the surface, (2) a dark spot, (3) a fine granules region, (4) the matrix. Table 8 indicated that the white spot contains 25.3% Nd, which is the highest among the sample points. But compared to the Nd-rich phase in Fig. 3 and Table 2, the weight percentage of Nd dropped by 22.2%. The dark spot on the surface contains 18.8 wt% O, indicating that oxidation had taken place on it. As the sample analysed in Fig. 8, no Pr is determined on the sample points. In addition, approximately 6 wt% carbon was detected on the surface, these carbon signals are supposed to be originated from hydrocarbon contamination. (Postek, 1996) It can be concluded that compared to the matrix, Nd-rich phase is more reactive, which matched Kumari (2022)'s finding, (Kumari, 2021) and Pr also shows high dissolution ability during electroleaching in citric acid.

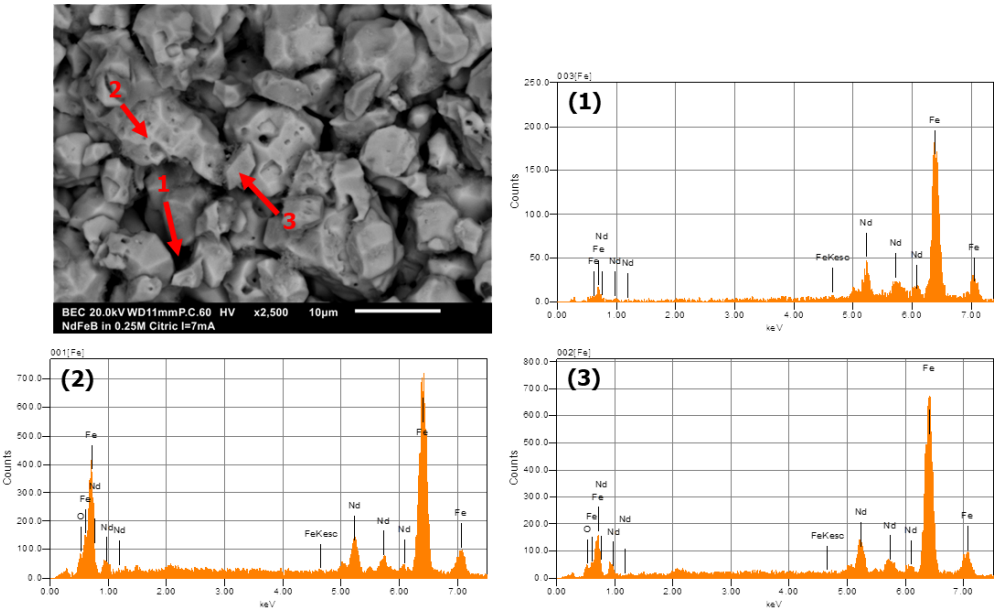

Fig. 10 SEM-EDS point analyses of chemical composition on a NdFeB magnet after CP measurement in 0.25 M citric acid under 7 mA/cm^2 current density for 133 s.

Table 7. Semi-quantitative chemical composition (wt%) detected by EDS point analyses 1-3 in Fig. 10

Element	1 (Cavity)	2 (White Matrix)	3 (Grey Spots)
Nd	26.6	22.2	23.3
Fe	73.4	76.0	75.1
O	/	1.9	1.6

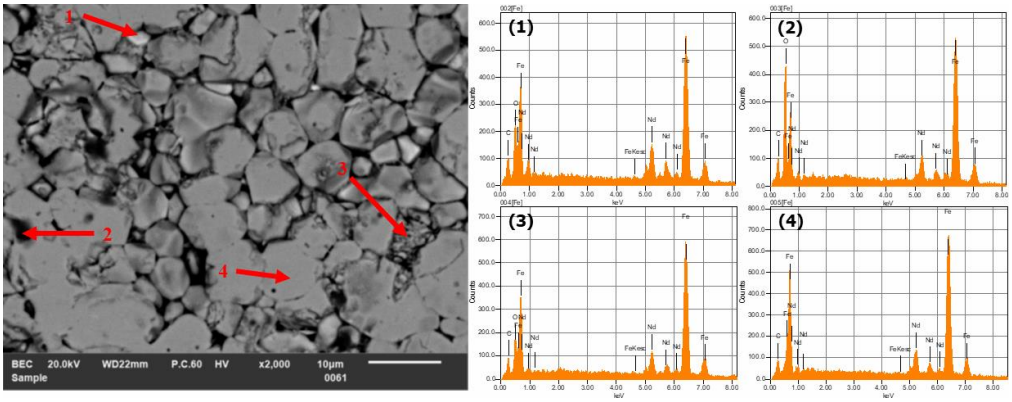

Fig. 11 SEM-EDS point analyses of chemical composition on a NdFeB magnet underwent LSV test after 5 min OCP measurement in 1 M citric acid.

Table 8. Semi-quantitative chemical composition (wt%) detected by EDS point analysis 1-4 in Fig. 11

Element	1 (White spot)	2 (Dark spot)	3 (Fine granules)	4 (Matrix)
Nd	25.3	17.0	20.2	20.7
Fe	60.7	57.5	66.9	73.3
O	8.2	18.8	6.8	/
C	5.8	6.7	6.1	6.1

Additionally, a EDS point analysis was conducted in a breakdown cavity region on a sample underwent LSV test after 5 min OCP measurement in 0.75 M citric acid, the detection presented the appearance of zirconium (Zr) and copper (Cu). No such elements were determined in the previous analysis. According to the principle of X-ray spectroscopy, the detector measures the energy of the emitted photons. (Hodoroaba, 2020) A hypothesis is suggested that some interference between the emitted photons took place in the cavity so that part of the biased photon energy of Nd (Mα1=0.97 keV) was recognized as the L- lines energy of Cu ($K_{\alpha1}$=8.05 keV, $K_{\alpha2}$=8.03 keV, L_{α}=0.93 keV, L_{β}=0.95 keV), then during the emission, the detector also treated two photons as one and doubled the energy, thus recognized part of the Cu signals as Zr ($K_{\alpha1}$=15.78 keV, $K_{\alpha2}$=15.69 keV, L_{α}=2.04 keV, L_{β} =2.12 keV) signals. (Lawrence Berkeley National Laboratory, 2009)

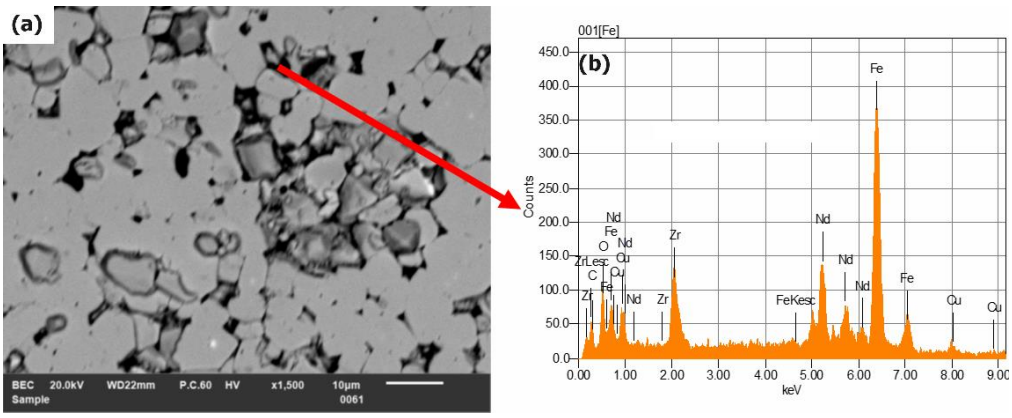

Fig. 12 SEM-EDS point analysis of chemical composition on a cavity on NdFeB magnet

underwent LSV test after 5 min OCP measurement in 0.75 M citric acid.

4. Conclusions

This study investigated the behaviour of spent NdFeB magnets from E-scooters during electroleaching in four biodegradable organic acids, in order to assist the selection for suitable electrolytes that promotes an environmentally friendly REE electroleaching. SEM-EDS characterization analysed the chemical composition of the sample and mapped the distribution of the elements and figured out the Nd-rich phases surrounded by the matrix. The coating layer of the magnet was stated to be made of Zn as well. OCP and LSV measurements are carried out for revealing the electrochemical behaviour of the organic acids, the reversed order of OCP values and corrosion current densities with regard to the pK_a values between acetic acid and formic acid revealed that the electroleaching behaviour among the organic acids are not only dictated by acidity. After comparison based on the corrosion current density and also took the cost into consideration, formic acid and citric acid are selected to study the effect of concentration on the anodic behaviour. The LSV tests for both acids resulted that the increasing concentration does not improve the corrosion current density all the way. Compared to formic acid, 0.25 M citric acid bear higher corrosion current density and lower pH value was eventually chosen as the agent for electroleaching. SEM characterization on the anodic polarization sites observed a rough and porous structure, and the increase in test time and acid concentration promotes the dissolution. SEM-EDS analysis of elemental composition revealed that the Nd-rich phases and Pr element show good dissolution ability during electroleaching in citric acid. Attributed to the voltage limit of the potentiostat, the chronopotentiometry test to discover the impact of external applied current density and the concentration of citric acid on the amount of dissolved material was unable to carry out. In further studies, potentiostats with broader voltage range will be equipped in order to achieve the experimental condition. Moreover, inductively coupled plasma - optical emission spectrometry (ICP-OES) technique is also planned to be utilized for evaluating the electroleaching efficiency as a function of acid concentration and current density. The result of this study aids the selection of proper reagents for Nd electroleaching process. As an alternative to hydrometallurgy, electroleaching using natural organic acids has obvious advantages in reducing poisonous contamination, excessive treatment and acid consumption and contributes to environmental friendliness. (Önal M. A., 2017) (Mao, et al., 2022) (Lyman & G.R., 1993) As more effort are putting in the research in REE recovery, the capability of eco-friendly industry can be eventually realised.

5. References

Agence Nationale de la Recherche. (2018, January). *Electroleaching-Electrodeposition For recovery of Precious metals from electrical / electronic equipments – EE4Precious*. Retrieved from anr.fr: https://anr.fr/Project-ANR-20-CE08-0035

Bandara, H. D. (2016). Rare earth recovery from end-of-life motors employing green chemistry design principles. *Green Chemistry*, 753-759. doi:10.1039/C5GC01255D

Belfqueh, S., Seron, A., Chapron, S., Arrachart, G., & Menad, N. (2023). Evaluating organic acids as alternative leaching reagents for rare earth elements recovery from NdFeB magnets. *Journal of Rare Earths*, 621-631. Retrieved from https://doi.org/10.1016/j.jre.2022.04.027

Chen, J. Y. (2022, Feburary). Rare earth passivation and corrosion resistance of zinc coated NdFeB magnets. *Journal of Rare Earths, 40*(2), 302-308. Retrieved from https://doi.org/10.1016/j.jre.2020.11.012

Erust, C., Akcil, A., Tuncuk, A., Deveci, H., & Yazici, E. Y. (2019). A Multi-stage Process for Recovery of Neodymium (Nd) and Dysprosium (Dy) from Spent Hard Disc Drives (HDDs). *Mineral Processing and Extractive Metallurgy Review, 42,2021*(2), 90-101. Retrieved from https://doi-org.tudelft.idm.oclc.org/10.1080/08827508.2019.1692010

Goldberg, R. N., Kishore, N., & Lennen, R. M. (2002). *Thermodynamic Quantities for the Ionization Reactions of Buffers.* Melville NY: AIP Publishing. Retrieved from https://doi-org.tudelft.idm.oclc.org/10.1063/1.1416902

Hamel, C., Chamelot, P., & Taxil, P. (2004). Neodymium (III) cathodic processes in molten fluorides. *Electrochimica Acta, 49*(25), 4467-4476. Retrieved from https://doi.org/10.1016/j.electacta.2004.05.003

Haynes, W. M. (2014). *CRC handbook of chemistry and physics.* Boca Raton: CRC press.

Hesami, R., Ahmadi, A., Hosseini, M. R., & Manafi, Z. (2022). Electroleaching kinetics of molybdenite concentrate of Sarcheshmeh copper complex in chloride media. *Minerals Engineering*, 107721. Retrieved from https://doi.org/10.1016/j.mineng.2022.107721

Hodoroaba, V. D. (2020). Energy-dispersive X-ray spectroscopy (EDS). In V. D. Hodoroaba, *Characterization of Nanoparticles* (pp. 397-417). Berlin: Elsevier. Retrieved from https://doi.org/10.1016/B978-0-12-814182-3.00021-3

IEA. (2021). *The Role of Critical Minerals in Clean Energy Transitions.* Paris: IEA. Retrieved from https://www.iea.org/reports/the-role-of-critical-minerals-in-clean-energy-transitions

Jakobsson, L. K., Tranell, G., & Jung, I.-H. (2016). Experimental Investigation and Thermodynamic Modeling of the B2O3-FeO-Fe2O3-Nd2O3 System for Recycling of NdFeB Magnet Scrap. *Metallurgical and Materials Transactions B*, 2017. Retrieved from https://doi.org/10.1007/s11663-016-0748-0

Jiang, Y., Deng, Y., Xin, W., & Guo, C. (2020). Oxidative Roasting–Selective Pressure Leaching Process for Rare Earth Recovery from NdFeB Magnet Scrap. *Transactions of the Indian Institute of Metals*, 703–711. doi:https://doi.org/10.1007/s12666-020-01888-x

Kliewer, W. M., Howarth, L., & Omori, M. (1967). Concentrations of tartaric acid and malic acids and their salts in Vitis vinifera grapes. *American Journal of Enology and Viticulture*, 42-54.

Kumari, A. R. (2021). Electrochemical treatment of spent NdFeB magnet in organic acid for recovery of rare earths and other metal values. *Journal of cleaner production*, 127393. Retrieved from https://doi.org/10.1016/j.jclepro.2021.127393

Lawrence Berkeley National Laboratory (2009). *X-ray Data Booklet.* Berkeley: University of California.

Lee, C. H. (2013). Selective leaching process for neodymium recovery from scrap Nd-Fe-B magnet. *Metallurgical and Materials Transactions A*, 5825-5833. doi:https://doi.org/10.1007/s11661-013-1924-3

Liu, S.L., Meng, J., Fan, H.R., Liu, X., Butcher, A. R., Yann, L., . . . Li, X.-C. (2023). Global rare earth elements projects: New developments and supply chains. *Ore Geology Reviews*, 105428. Retrieved from https://doi.org/10.1016/j.oregeorev.2023.105428

Lyman, J., & G.R., P. (1993). Recycling of rare earths and iron from NdFeB magnet scrap. *High Temperature Materials and Processes*, 175-188.

Makarova, I. S. (2020). Electrochemical leaching of rare-earth elements from spent NdFeB magnets. *Hydrometallurgy*, 105264. Retrieved from https://doi.org/10.1016/j.hydromet.2020.105264

Mao, F., Zhu, N., Zhu, W., Liu, B., Wu, P., & Dang, Z. (2022). Efficient recovery of rare earth elements from discarded NdFeB magnets by mechanical activation coupled with acid leaching. *Environmental Science and Pollution Research, 29*, 25532-25543. Retrieved from https://doi.org/10.1007/s11356-021-17761-3

Mishra, R. K. (1987). Microstructure of hot-pressed and die-upset NdFeB magnets. *Journal of applied physics*, 967-971. Retrieved from https://doi-org.tudelft.idm.oclc.org/10.1063/1.339709

Omodara, L. P. (2019). Recycling and substitution of light rare earth elements, cerium, lanthanum, neodymium, and praseodymium from end-of-life applications-A review. *Journal of Cleaner Production*, 117573. Retrieved from https://doi.org/10.1016/j.jclepro.2019.07.048

Önal, M. A. (2015). Recycling of NdFeB magnets using sulfation, selective roasting, and water leaching. *Journal of Sustainable Metallurgy*, 199-215. Retrieved from https://doi.org/10.1007/s40831-015-0021-9

Önal, M. A. (2017). Recycling of NdFeB magnets using nitration, calcination and water leaching for REE recovery. *Hydrometallurgy*, 115-123. Retrieved from https://doi.org/10.1016/j.hydromet.2016.11.006

Papagianni, M. (2007). Advances in citric acid fermentation by Aspergillus niger: Biochemical aspects, membrane transport and modeling. *Biotechnology Advances*, 244-263. Retrieved from https://doi.org/10.1016/j.biotechadv.2007.01.002

Postek, M. T. (1996). An approach to the reduction of hydrocarbon contamination in the scanning electron microscope. *Scanning, 18*(4), 269-274. Retrieved from https://doi-org.tudelft.idm.oclc.org/10.1002/sca.1996.4950180402

Smith, R. M., & Martell, A. E. (1989). *Critical stability constants: second supplement.* New York: Springer New York. Retrieved from https://doi.org/10.1007/978-1-4615-6764-6

Sueptitz, R., Uhlemann, M., Gebert, A., & Schultz, L. (2010, March). Corrosion, passivation and breakdown of passivity of neodymium. *Corrosion Science, 52*(3), 886-891. Retrieved from https://doi.org/10.1016/j.corsci.2009.11.008

Suzuki, I., Hisamatsu, Y., & Masuko, N. (1980). Nature of atmospheric rust on iron. *Journal of the Electrochemical Society*, 2210.

The Business Research Company. (2023, January). *The Business Research Company*. Retrieved from Rare Earth Metals Global Market Report:

https://www.thebusinessresearchcompany.com/report/rare-earth-metals-global-market-report

Trummal, A., Lipping, L., Kalijurand, I., Koppel, I. A., & Leito, I. (2016). Acidity of Strong Acids in Water and Dimethyl Sulfoxide. *The Journal of Physical Chemistry A*, 3663-3669. doi:10.1021/acs.jpca.6b02253.

van der Hoogerstraete, T., Blanpain, B., van Gerven, T., & Binnemans, K. (2014). From NdFeB magnets towards the rare-earth oxides: a recycling process consuming only oxalic acid. *RSC Advances*, 64099-64111. doi:10.1039/C4RA13787F

Vandarkuzhali, S., Chandra, M., Ghosh, S., Samanta, N., Nedumaran, S., Reddy, B. P., & Nagarajan, K. (2014). Investigation on the electrochemical behavior of neodymium chloride at W, Al and Cd electrodes in molten LiCl-KCl eutectic. *Electrochimica Acta, 145*, 86-98. Retrieved from https://doi.org/10.1016/j.electacta.2014.08.069

Vander Hoogerstraete, T., Blanpain, B., Van Gerven, T., & Binnemans, K. (2014). From NdFeB magnets towards the rare-earth oxides: a recycling process consuming only oxalic acid. *RSC Advances, 4*(109), 64099-64111. Retrieved from https://doi-org.tudelft.idm.oclc.org/10.1039/C4RA13787F

Venkatesan, P. S. (2018). An environmentally friendly electro-oxidative approach to recover valuable elements from NdFeB magnet waste. *Separation and Purification Technology*, 384-391. Retrieved from https://doi.org/10.1016/j.seppur.2017.09.053

Venkatesan, P. V. (2018). Selective electrochemical extraction of REEs from NdFeB magnet waste at room temperature. *Green chemistry*, 1065-1073. doi:10.1039/C7GC03296J

von Harrach, H., Klenov, D., Freitag, B., Schlossmacher, P., Collins, P., & Fraser, H. (2010). Comparison of the detection limits of EDS and EELS in S/TEM. *Micoscopy and Microanalysis*, 1312-1313. Retrieved from https://doi-org.tudelft.idm.oclc.org/10.1017/S1431927610058940

Yang, Y., Zhao, R., & Zhao, Z. (2021). Electrochemical behaviors of neodymium ions on a solid iron electrode in molten lithium fluoride and reaction kinetics of forming Nd2Fe17 intermetallic compound. *Separation and Purification Technology, 257*, 117882. Retrieved from https://doi.org/10.1016/j.seppur.2020.117882

Yoon, H.S., Kim, C.J., Chung, K., Lee, S.J., Joe, A.R., Shin, Y.H., . . . Kim, J.G. (2014). Leaching kinetics of neodymium in sulfuric acid from E-scrap of NdFeB permanent magnet. *Korean Journal of Chemical Engineering*, 706-711. Retrieved from https://doi.org/10.1007/s11814-013-0259-5